Molecular Dynamics Investigation of an Oriented Cyclic Peptide Nanotube in DMPC Bilayers

Mounir Tarek, Bernard Maigret, and Christophe Chipot
Equipe de Dynamique des Assemblages Membranaires, Unité Mixte de Recherche CNRS/UHP 7565, Institut Nancéien de Chimie Moléculaire, Université Henri Poincaré, B.P. 239, 54506 Vandœuvre-lès-Nancy Cedex, France

ABSTRACT Nanotubes resulting from the self-assembly of cyclic peptides formed by eight α-amino acids and inserted into lipid bilayers have been shown to function as synthetic, integral transmembrane channels. A nanotube consisting of eight *cyclo*[(L-Trp-D-Leu)$_3$-L-Gln-D-Leu] subunits, organized in an antiparallel, β-sheetlike channel embedded in a hydrated dimyristoylphosphatidylcholine bilayer was investigated in an 8-ns molecular dynamics trajectory. This large-scale statistical simulation brings to light not only the atomic-level structural features of the synthetic channel, but also its dynamical properties. Overall, the nanotube conserves its hollow tubular structure. The calculation reproduces the tilt of the channel with respect to the normal of the bilayer, in reasonable agreement with experiment. The results show a dislocation of the nanotube indicative of a possible disassembly process that may influence the channel conduction. The dynamics of the water in the hollow tubular structure has been characterized, and the conductance of the channel has been estimated. Transport properties of the peptide nanotube are discussed in comparison with other transporters.

INTRODUCTION

The increase of bacterial resistance to a wide range of therapeutic agents, and hence of the proliferation of bacterial infections, has motivated the development of original drugs capable of responding effectively to these new contingencies. It has been shown recently that cyclic peptides featuring an even number of alternating L and D α-amino acids act preferentially on the membrane of Gram-positive and Gram-negative bacteria, with respect to mammalian cells, by increasing in a significant manner its permeability and causing its fast depolarization, thereby leading to a rapid death of the cell (Fernandez-Lopez et al., 2001). Cyclic peptides formed by L and D α-amino acids are easy to synthesize, are proteolytically stable, and, under appropriate conditions, self-assemble into hollow, tubular structures by means of a network of hydrogen bonds that connect the stacked subunits (Bong et al., 2001; Ghadiri et al., 1993). The unique architecture of this synthetic channel, integral to the lipid bilayer, and its rapid bactericidal action suggest that such self-organized systems could constitute a potent alternative to conventional antibiotics and an effective candidate to reduce bacterial resistance.

Cyclic peptides that form quasi-β-strands self-organize in a network of hydrogen bonds between the oxygen atoms of the participating carbonyl groups and the hydrogen atoms of the amino groups. On account of the alternated L/D chirality of the amino acids, the lateral chains are oriented toward the outside of the channel. The resulting internal structure of the intermolecular pore, lined by carbonyl and amide dipoles, resembles that of gramicidin A (Arseniev et al., 1985; Ketchem et al., 1997; Roux, 2002). Electron diffraction patterns, x-ray, and Fourier transform infrared spectroscopy analyses indicate that the tightly hydrogen-bonded rings stack with an average intersubunit distance of ~4.7 Å (Hartgering et al., 1996; Ghadiri et al., 1993). Depending upon the sequence of the cyclic peptide subunit, the resulting nanotubes can adopt different modes of membrane permeation. The simplest supramolecular organization is a single cylindrical structure embedded in the lipid bilayer, with a transmembrane orientation, i.e., with its central axes approximately perpendicular to the membrane (Ghadiri et al., 1994; Kim et al., 1998). Nanotubes can also self-assemble within the membrane, in the direction parallel to the water-bilayer interface (Fernandez-Lopez et al., 2001). This so-called ''carpetlike'' mode of membrane permeation is thought to exhibit a greater potential for membrane discrimination due to the larger possibilities of hydrophilic interactions of lipid headgroups with the participating polar side chains. Alternatively, peptide nanotubes can self-assemble into complex multimeric entities that constitute nanopores, or ''barrel staves.'' Just like multihelix transmembrane proteins, these nanopores result from the association of individual nanotubes through favorable interactions of their polar residues—constituting the hydrophilic interior of the pore—whereas the nonpolar ones are exposed to the aliphatic chains that form the hydrophobic core of the lipid bilayer.

Just like for a wide variety of functionalized model channels, including β-barrels with a polybenzene backbone, bolaamphiphiles, and cyclodextran rings with lipid chains (Matile, 2001; Cragg, 2002), several investigations have revealed that peptide nanotubes may act as highly selective and efficient transmembrane channels for ions and small molecules. Structures consisting of eight (Ghadiri et al.,

Submitted September 25, 2002, and accepted for publication May 29, 2003.

Address reprint requests to Mounir Tarek, Equipe de Dynamique des Assemblages Membranaires, Unité Mixte de Recherche CNRS/UHP 7565, Institut Nancéien de Chimie Moléculaire, Université Henri Poincaré, B.P. 239, 54506 Vandœuvre-lès-Nancy Cedex, France. E-mail: mtarek@edam.uhp-nancy.fr.

© 2003 by the Biophysical Society

0006-3495/03/10/2287/12 $2.00

1993, 1994), 10 (Granja and Ghadiri, 1994), and 12 (Khazanovich et al., 1994) cyclic peptide subunits form tubular structures with the diameter of the internal van der Waals pore estimated to be 7, 10, and 13 Å, respectively. These structures have been shown to be large enough to serve as a conduit for water (Engels et al., 1995), function as size-selective ion channels (Ghadiri et al., 1994; Motesharei and Ghadiri, 1997; Asthagiri and Bashford, 2002), and mediate the transport of biologically relevant molecules, such as glucose, across the lipid bilayer (Granja and Ghadiri, 1994).

From a theoretical standpoint, cyclic peptide nanotubes potentially constitute ideal candidates for investigating the transport of water, ions, and small molecules. This complements our understanding of the general transport phenomena through model systems such as carbon nanotubes (Hummer et al., 2001) or through model geometries (Yang et al., 2002) where confinement plays an important role. Peptide nanotubes present the particularity of being similar both in function and shape to channels formed by natural proteins and peptide assemblies, yet are characterized by a semirigid hydrophilic pore structure. Conformational dynamics of natural channels appears to be often necessary to ensure or regulate the transport of molecular or ionic substances (Zhu et al., 2001; Kong and Ma, 2001; Forrest et al., 2000; Zhong et al., 1998). Characterization of this dynamics and its effects on the transport properties of a given channel using modeling techniques, such as molecular dynamics simulations, is far from being an easy task. This is due, in part, to the slow relaxation of the surrounding lipid molecules that is known to be in the order of tens to hundreds of nanoseconds (König and Sackmann, 1996; Feller et al., 1999). Moreover, the dynamics of the protein itself may cover the same timescale, which nowadays remains difficult to access within reasonable simulation times.

In this contribution, we consider a single synthetic channel resulting from the stacking of eight peptide subunits of sequence *cyclo*[(L-Trp-D-Leu)$_3$-L-Gln-D-Leu], embedded in a fully hydrated dimyristoylphosphatidylcholine (DMPC) bilayer. This system has been investigated (Kim et al., 1998) using polarized attenuated total reflectance infrared (ATR-IR) spectroscopy. It was shown that the nanotube orients itself in a transport-competent membrane orientation. Here, we examine the structural characteristics of the synthetic channel and its transport properties using state-of-the-art, large-scale molecular dynamics (MD) simulations over 8 ns. The results complement earlier theoretical investigations of water and ion transport in peptide nanotubes in the absence of the lipid environment (Engels et al., 1995; Asthagiri and Bashford, 2002). In the following section, the model system adopted for this study and the methodological aspects of the calculations are described. Next, the results of the MD simulation are presented, emphasizing the transport properties of the synthetic channel and the effect of the nanotube on the lipid structure.

METHODS AND COMPUTATIONAL DETAILS

Description of the system

The system consists of one nanotube inserted in a fully hydrated DMPC bilayer, in accord with Kim et al. (1998). The nanotube formed by eight *cyclo*[(L-Trp-D-Leu)$_3$-L-Gln-D-Leu] subunits was built using the ACCELRYS visualization package InsightII (San Diego, CA). In vesicles, single-channel conductance experiments show that, for a particular sequence of α-amino acids, nanotubes with different numbers of rings may assemble in the bilayer (Ghadiri et al., 1994). There is no indication from experiment what is the exact number of cyclic peptides that constitute the channel in multilamellar stacks of DMPC bilayers. Single-channel conductance experiments suggest for that particular sequence of α-amino acids that the number of rings be comprised between eight and 10 (Ghadiri et al., 1994). Here we have chosen to consider an assembly of eight peptide subunits to roughly coincide with the thickness of the hydrophobic core of the DMPC bilayer. A cyclic peptide was constructed preliminarily, so that its carbonyl, C=O, and its amino, N–H, chemical bonds be normal to the plane of the ring. On account of the alternated L and D chirality, all side chains of the peptide point outward. The χ torsional angles were chosen to warrant the flattest possible conformation of the ring. The cyclic peptides were stacked in such a fashion that 1), the L-Trp and the D-Leu side chains be distributed uniformly, and 2), eight intersubunit backbone-backbone hydrogen bonds be formed between two consecutive rings (Fig. 1). The backbone-backbone intermolecular hydrogen bonding interactions were optimized considering an antiparallel β-sheetlike stacked arrangement of the rings, in agreement with experiment (Ghadiri et al., 1993; Hartgering et al., 1996). According to Ghadiri et al. (1994), the L-glutamine residue is used mainly to simplify peptide synthesis. The system should therefore have the same characteristics as that formed by *cyclo*[(L-Trp-D-Leu)$_4$] subunits, for which, on account of the D-L chirality and the antiparallel β-sheetlike stacked arrangement, all rotational isomers are identical. In the sequence used here, the presence of L-Gln residues may lead to topoisomers. The latter were considered while setting up the system. L-Gln residues were placed in consecutive rings either on the same or on opposite sides (Fig. 1 *d*). The results presented below show that the ring-to-ring structural features are conserved in both cases. In the following the nanotube rings are numbered 1 to 8 as displayed in Fig. 1.

The membrane used for this study was constructed from an equilibrated fully hydrated DMPC bilayer containing 64 lipid units and 1,645 water molecules. At the temperature set for the study, i.e., 30°C, the bilayer is in the biologically relevant liquid crystal Lα phase. The system is characterized by a surface area of ~60 Å^2 per lipid, and a lamellar spacing of ~61 Å, which falls within 2% of the experimental values (Petrache et al., 1998). This system was replicated ($2x \times 2y$) in the plane of the bilayer. The nanotube was inserted at the center of the bilayer with its long axis normal to the interface (Fig. 2 *a*). Overlapping lipid and water molecules were discarded to avoid poor van der Waals interactions. The complete system (synthetic channel, 215 lipid units, and 6,469 water molecules) represented a total of 46,097 atoms. The initial dimensions of the simulation cell were $98 \times 78.5 \times 61$ Å^3. Periodic boundary conditions were applied in all three directions of space.

Several approaches can be adopted to equilibrate the simulation box. A common one consists in freezing the degrees of freedom of the protein, while the lipid bilayer and the water molecules optimize their interactions with the latter (Chiu et al., 1999; Shrivastava and Sansom, 2000; Bernèche and Roux, 2000; Elmore and Dougherty, 2001; De Groot and Grubmüller, 2001). We chose to leave the synthetic channel unconstrained, allowing the peptide units to adjust their position in the direction perpendicular to the plane of the lipid bilayer and relax the constituent side chains for optimal packing with the surrounding hydrocarbon chains. No water molecules were initially placed inside the nanotube.

Molecular dynamics simulation

The MD simulation presented here was carried out using the program NAMD version 2.4 targeted for massively parallel architectures (Kale et al.,

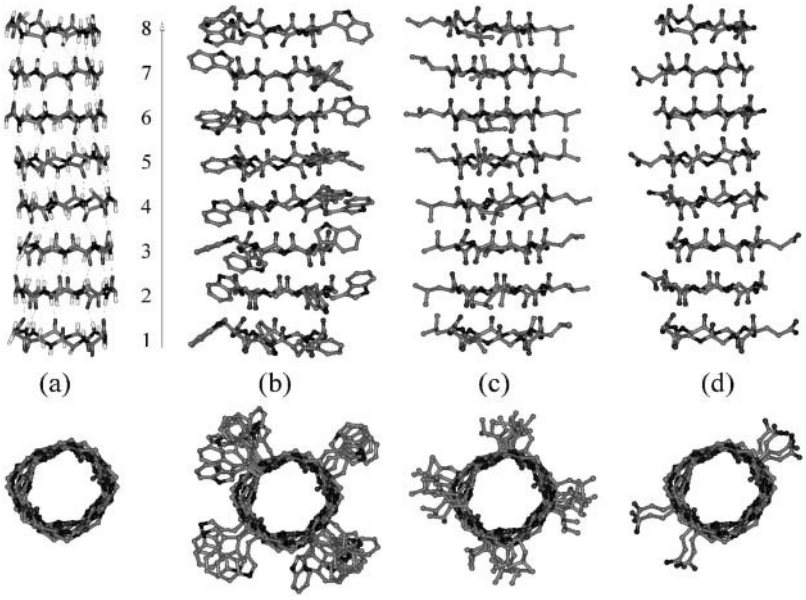

FIGURE 1 Initial configuration adopted for the synthetic channel, resulting from the self-assembly of eight *cyclo*[(L-Trp-D-Leu)$_3$-L-Gln-D-Leu] peptides through a network of intersubunit backbone-backbone hydrogen bonds. (*a*) On account of the alternated L and D chirality, all the side chains are pointing outward from the synthetic channel, and except for Gln, there are no other conformers resulting from the rotation of the rings with respect to each other (the distribution of the L-Trp (*b*) and D-Leu (*c*) side chains is unique). The topoisomers were chosen so that the L-Gln side chains in consecutive rings are oriented in opposite sides except between the fourth and the fifth rings (*d*). The rings are numbered 1–8.

1999; Bhandarkar et al., 2002). The system was examined in the (N, P, T) ensemble, wherein the dimensions of the cell in the three directions of space fluctuate independently. The equations of motion were integrated using a multiple time-step algorithm (Martyna et al., 1996; Izaguirre et al., 1999, 2001). A time step of 1.0 fs was employed. Short- and long-range forces were calculated every two and four time steps, respectively. A Langevin piston maintained the pressure of the cell at 1 atm, and Langevin dynamics was used to control the temperature at 300 K. Chemical bonds between hydrogen and heavy atoms were constrained to their equilibrium value by means of the SHAKE/RATTLE algorithm (Ryckaert et al., 1977; Andersen, 1983). Long-range, electrostatic forces were taken into account using a fast implementation of the particle mesh Ewald approach (Darden et al., 1993; Essmann et al., 1995), with a direct space sum tolerance of 10^{-6} and a spherical truncation of 11 Å. The reciprocal space contribution of the Coulomb sum was evaluated on a grid of $98 \times 81 \times 61$ points, with a cubic spline interpolation of the charges.

The water molecules were described using the TIP3P model. Bond stretching, valence angle deformation, and torsional and nonbonded parameters of the cyclic peptides forming the nanotube and of the DMPC lipid units were extracted from the all-atom CHARMM force field (MacKerell et al., 1998). Execution of NAMD2 was performed on 32 R14000 (500 MHz) processors of an SGI Origin 3800 (Mountain View, CA).

RESULTS AND DISCUSSION

Overall features of the system

As already mentioned, the cavity created in the hydrated DMPC bilayer to accommodate the peptide channel has been slightly oversized to prevent deleterious van der Waals interactions. During the first 3 ns of the run (Fig. 3), the dimensions of the simulation cell adjusted to yield an optimal surface area and thickness, before stabilizing for the remaining 4 ns (Fig. 3). As can be seen in Fig. 2, during the run water molecules have spontaneously diffused in the hollow cylindrical channel. Overall, the antiparallel, β-sheetlike structure of the nanotube appears to be well conserved, with minimal distortion in the conformation of the participating peptide rings. Finally, as expected, the synthetic channel has tilted with respect to its original orientation.

Characteristics of the nanotube

The initial and final conformations of the channel are reported in Fig. 4. The original orientation is modified within the first 2 ns of the trajectory. Toward 3.0 ns, the first two cyclic peptides returned to their initial position, causing a kink in the nanotube. The second and third rings remained, however, interdependent by means of reminiscent hydrogen bonds that act as a hinge. The network of hydrogen bonds in the last six rings appears to be intact and unaffected by the kink. In the course of the simulation, the dynamic reorientation of the side chains led to the formation of intersubunit side chain-side chain hydrogen bonds, in particular between L-Trp and L-Gln.

Full analysis of the nanotube orientation with respect to the normal of the membrane (n) is presented in Fig. 5. Fig. 5 *a*, reporting the tilt of the longitudinal axis (Zn) of the channel, highlights a stable plateau $\sim$15° reached within 2 ns. Use of the longitudinal axis to measure the nanotube tilt with respect to n yields an average orientation. In contrast, ATR-IR spectroscopy probes the amide N–H and C=O bonds orientations (Ghadiri et al., 1994; Kim et al., 1998). We report in Fig. 5 *b* the probability distribution of the angle formed by the participating N–H and C=O bonds and n, averaged over the individual rings and over the last nanosecond of the simulation. Roughly speaking, the tilt angle of the amide moieties peaks $\sim$15°, but presents a rather large distribution. The average angle between the amide moieties and n amounts to 25°. This value is underestimated when compared to the ATR-IR spectroscopy measurements, which predict a tilt of 39°, based on the amide I transition.

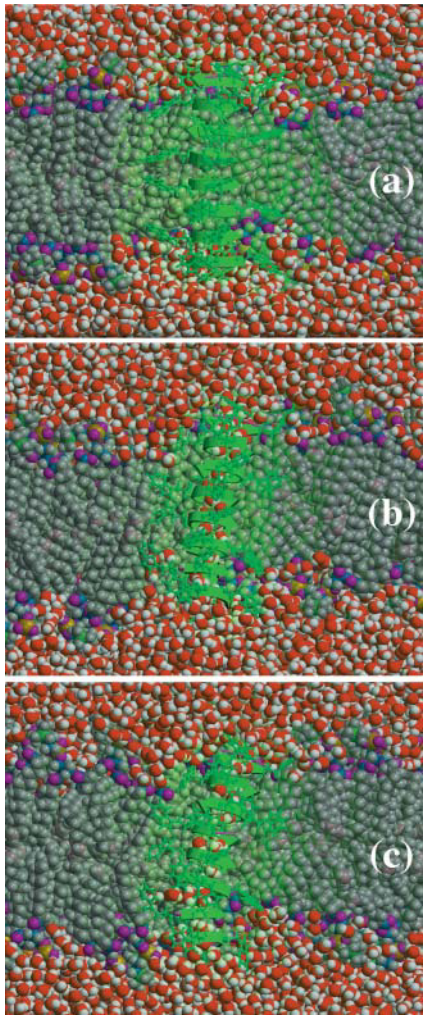

FIGURE 2 Instantaneous configurations taken from the MD trajectory for (*a*) the initial system ($t = 0$ ns), (*b*) at $t = 2.8$ ns, and (*c*) at the end of the 8.0-ns NPT run. A cartoon representation is used to show the eight rings forming the antiparallel, β-sheetlike channel (*green*). Water (O, *red*; H, *white*) and DMPC (C, *dark gray*; DMPC H, *light gray*; N, *green*; P, *yellow*; and O, *purple*) atoms are rendered with the appropriate atomic van der Waals radii. The L-Trp side chains of the nanotube are displayed in ball-and-stick representation. The image was generated employing MOLSCRIPT (Kraulis, 1991) and RASTER3D (Bacon and Anderson, 1988; Merritt and Murphy, 1994).

Not too unexpectedly, larger amplitudes can be witnessed for the first and the second subunits, on account of the opening of the channel. From a more general perspective, as displayed in Fig. 5, *c* and *d*, the rings located at the end of the nanotube exhibit a greater flexibility. Consequently, the tilt of their amide groups is more pronounced and more mobile than for those rings well inside the cylindrical structure—viz. fourth and fifth cyclic peptides.

To appreciate how the inner structure of the synthetic channel is conserved throughout the MD simulation, the density profiles of all backbone atoms were determined along *Zn* (Fig. 6). These were calculated as time-averages of

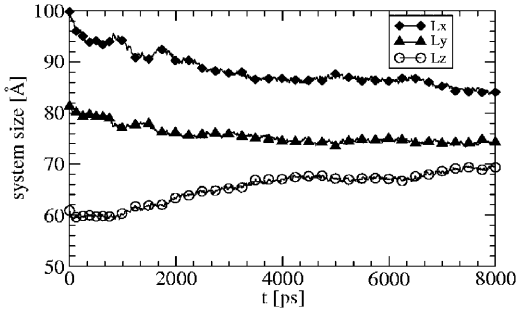

FIGURE 3 Evolution of the dimensions of the simulation cell along the MD trajectory. z is the direction normal to the water-bilayer interface. Contraction of the system in the x and y directions is suggestive of an improved packing of the DMPC lipid chains around the peptide channel.

200 ps, at 1-ns intervals. The sharpness of the peaks provides a valuable measure of the flatness of each participating cyclic peptide. The first peak remains reasonably well resolved until ~3.0 ns, after which the profiles representing the first and the second rings coalesce. This coincides with the opening of the nanotube and stems from the reorientation of the first two cyclic peptides along the normal to the water-bilayer interface. At the same time, the density profiles of the last six rings remain particularly sharp, suggesting that the cyclic peptides are perfectly flat. The distance separating the peaks, i.e., the intersubunit distance, estimated on average to be 4.85 ± 0.15 Å, is also very well conserved and concurs with the value determined from electron diffraction patterns, x-ray analyses, and estimates from IR measurements (Hartgering et al., 1996; Ghadiri et al., 1993).

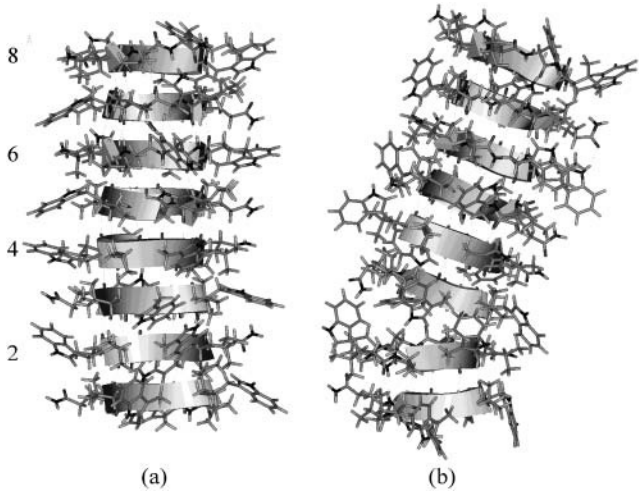

FIGURE 4 Organization of the eight *cyclo*[(L-Trp-D-Leu)$_3$-L-Gln-D-Leu] peptides forming the synthetic channel at (*a*) $t = 1$ ns, and (*b*) $t = 8$ ns. In the first arrangement, all the rings are flat and perfectly stacked. The longitudinal axis of the nanotube is almost aligned with the normal to the water-bilayer interface. In the second arrangement, the nanotube exhibits a kink between the second and the third rings (from bottom to top), conserving the expected tilt for the last six cyclic peptides.

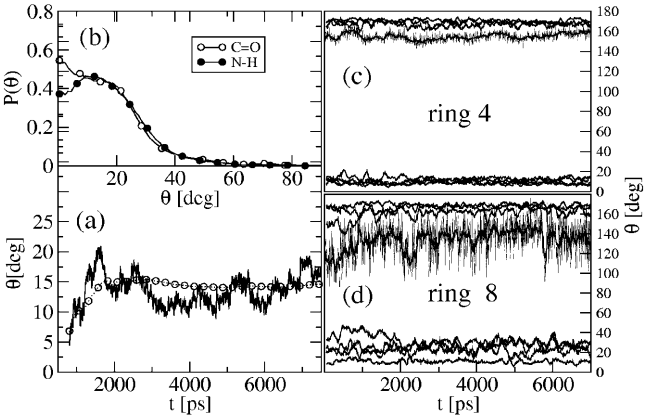

FIGURE 5 Orientation of the channel. (*a*) Time evolution of angle θ formed by the longitudinal axis *Zn* of the nanotube and the normal *n* to the water-bilayer interface, using all the atoms of the nanotube (*solid line*), and only the backbone atoms of the last six cyclic peptides (*open circles*); (*b*) Angular distribution of the C=O and N–H dipoles with respect to *n* averaged over all peptide units (upward and downward orientations are considered to be identical), during the last nanosecond of the MD run; (*c*) Time evolution of the angle formed by the 8 individual C=O bonds and *n* for ring 4 (located in the middle of the synthetic channel); and (*d*) for the outermost ring 8. A finer time grid representation is adopted for one selected C=O bond to highlight the fluctuations in θ.

As has been commented on earlier, self-assembly of the cyclic peptides into a synthetic channel proceeds through the formation of eight intersubunit backbone-backbone hydrogen bonds. Translocation of water molecules within the channel is accompanied by an intermittent breaking (10–50 ps) of the intersubunit hydrogen bonds. During these events, C=O and N–H chemical bonds slightly tilt to allow the formation of transient water-backbone hydrogen bonds, similar to that observed for aquaporins (Tajkhorshid et al., 2002) and gramicidin (Pomès and Roux, 2002). As a result, the ring-to-ring optimal hydrogen bonding is mediated by the presence of the water and is shown to disrupt intermittently

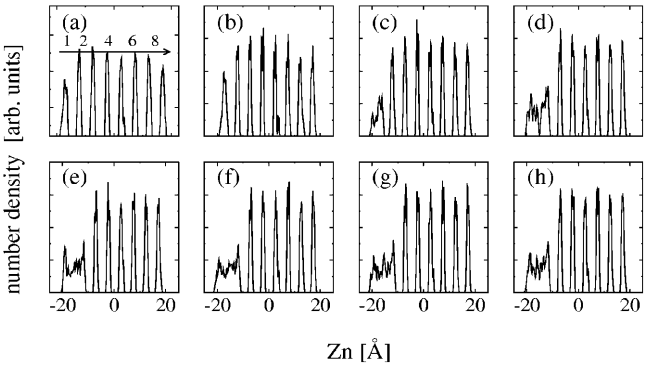

FIGURE 6 Number density profiles of the cyclic peptides based on their backbone atoms only, along the longitudinal axis (*Zn*) of the channel limited to its last six rings. The different sets of profiles are 1 ns apart, and correspond to time-averages of 200 ps. The rings are numbered from 1 to 8 (*a*).

up to three hydrogen bonds formed between neighboring rings. These fluctuations do not perturb significantly the overall ring-to-ring interactions, as their average distance remains close to 4.7 Å.

Structural and dynamical features of the water wire

The formation of a complete water column inside the peptide nanotube occurred after ~800 ps. Thereafter, the number of water molecules within the channel averaged to 21 molecules, with large fluctuations encompassing ±7 molecules (Fig. 7 *a*). Fluctuations of this nature have been observed previously in an MD simulation investigation of a nanotube immersed in water (Engels et al., 1995). In Fig. 7 *b*, we report the location of all water molecules that entered the nanotube during the last seven nanoseconds of the simulation. This figure shows that the distribution of the water molecules is not uniform, but rather, as previously found by Engels et al. (1995), presents higher densities in the regions between the planes of cyclic peptide. The empty hydration domains, for instance, ~2.5 ns between rings 3 and 4, and ~4.5–5.0 ns between rings 5 and 7, span lifetimes ranging from a few ten to a few hundred picoseconds. This is suggestive that the water column inside the tube is temporarily broken, a phenomenon also observed in the aquaporin-1 channel (De Groot and Grubmüller, 2001).

Whereas beyond the transitory regime an average of 21 water molecules fill the hollow cylindrical structure, a far greater number enter and leave the nanotube. During the last

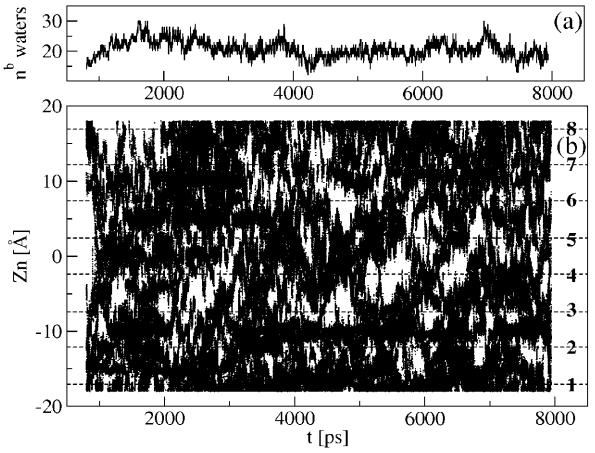

FIGURE 7 (*a*) Time evolution of the number of water molecules in the nanotube. Molecules are tallied if their oxygen atom lies between the two planes formed, respectively, by the first and the last cyclic peptides (*b*) Time evolution of the location of all water molecules that entered the ring during the last seven nanoseconds of the MD run. Note the higher density of water in those regions located between the planes (*horizontal broken lines*) formed by the constituent C_α carbon atoms of the rings (numbered 1–8 in *b*), and the sporadic empty domains (zero density) at several locations and different times.

seven nanoseconds of the MD run, >230 molecules ''visited'' the synthetic channel, i.e., diffused from beyond the outermost peptide rings toward the interior of the nanotube. The residence time of the participating water molecules can vary significantly. The motion of a selection of water molecules along the long axis of the channel depicted in Fig. 8 shows that some molecules may remain for several nanoseconds in the cylindrical structure. In contrast, others may reside very briefly in the cavity, generally in the vicinity of its opening. No directional flow of water molecules is observed; instead, water molecules appear to follow a random diffusion mode, from one residence site to another. The width of the channel, approximately equal to 7 Å, is large enough to accommodate more than a single-column water wire; whereas inside the nanotube the molecules form hydrogen bonds (Fig. 9 *a*) either 1), with the peptide subunits exclusively, 2); with other water molecules only; or 3), with both, as illustrated by molecule types 1, 2, and 3, respectively. Snapshots displayed in Fig. 9 *b* at different points along the trajectory emphasize the diversity of molecular organization. The figure shows that water molecules may adopt a variety of conformations to bridge rings 2 and 3 through complex hydrogen bonding networks, hence contributing to the overall stability of the peptide nanotube.

Whereas the present MD simulation does not reveal any clear-cut directional flow of water in the channel, the participating water molecules located inside the nanotube tend to adopt a preferential orientation. In Fig. 10, we report the time evolution of the orientation of the water molecular dipole with respect to *Zn*, for all water molecules that entered the cavity during the MD simulation. One peculiar feature shared by most of those water molecules is their similar orientation, the angle formed by their molecular dipole moment and the principal axis of the synthetic channel being

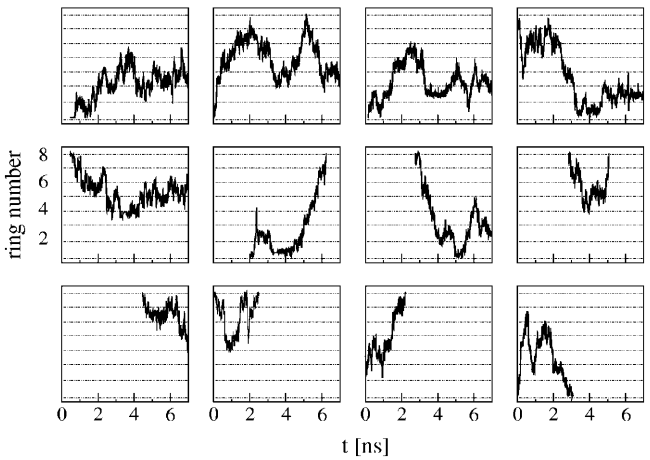

FIGURE 8 Schematic representation of the position of selected water molecules inside the peptide nanotube during the MD trajectory. The horizontal broken lines indicate the planes formed by the C_α carbon atoms of the participating rings.

either between 0 and 60°, or between 120 and 180°. In the course of the run, reorientation from one direction to the other occurs several times, in a concerted fashion. Sharp transitions like the one occurring at ~3.4 ns indicate that complete reorientation may proceed over very short timescales, i.e., less then 50 ps. Similar collective reorientations, suggestive of a ''two-state'' mechanism, have been reported for water wires in gramicidin (Chiu et al., 1999; Pomès and Roux, 2002).

The interaction of water molecules with the channel and their confinement does necessarily affect their dynamics. Estimates from the MD trajectory show that the translational diffusion coefficient for those molecules that are located in the tube (D_{pore}) is four times smaller than the diffusion coefficient in the bulk (D_{bulk}), based on a control simulation using the same forcefield and methodology. This result is similar to that found for the hydrated *cyclo*[(L-Gln-D-Ala)$_4$] channel (Engels et al., 1995). It indicates that cyclic octapeptide channels conduct water at a ratio $R_{\text{D}} = D_{\text{bulk}}/D_{\text{pore}}$ similar to that of channels formed by transmembrane helix bundles (Tieleman et al., 2001). For instance, simulations of synthetic tetrameric channels (Zhong et al., 1998) and pentameric M2 δ nicotinic receptors (Law et al., 2003) indicate that water within the pore lumen is slowed down by factors of 3 and 4, respectively. On the contrary, for transmembrane proteins with smaller pore sections such as *Escherichia coli* aquaglyceroporin GlpF (Tajkhorshid et al., 2002) and gramicidin (Chiu et al., 1999), R_{D} is found to be much smaller, viz. ~10. The exact behavior of water in channels extracted from simulations depends on the water model and the treatment of the environment, such as the explicit representation of the lipid matrix versus a constrained isolated channel (Tieleman et al., 2001). There is, however, a clear picture that emerges from results compiled for a variety of systems, including cylindrical cavities, simple model pores, or synthetic channels (Tieleman et al., 2001). It shows a correlation between the radius of the pore and R_{D}, to which the results for the peptide nanotube fit well.

Based on the pore dimension it is also possible to estimate the conductance of the channel (Smart et al., 1997; Smart et al., 1998). The method consists of approximating the conductance by integrating the electrical resistance of equivalent electrolyte-filled cylinders along the length of the channel and correcting for the reduced mobility of ions within the narrow pore. Using this approach encoded in the HOLE program (Smart et al., 1993), the conductance for the octapeptide nanotube, in its closed state, is found to be ~150 pS in 1 M KCl. This would correspond to 75 pS in 0.5 M KCl, which is comparable to the experimental conductance of 65 pS measured by Ghadiri et al. (1994). Interestingly enough, the rate of channel-mediated transport for K^+ ions estimated from the conductance measurements is three times faster than that of gramicidin A (Ghadiri et al. 1994). Similarly, the ratio of the translational diffusion coefficients of water in gramicidin A and in the nanotube is equal to three.

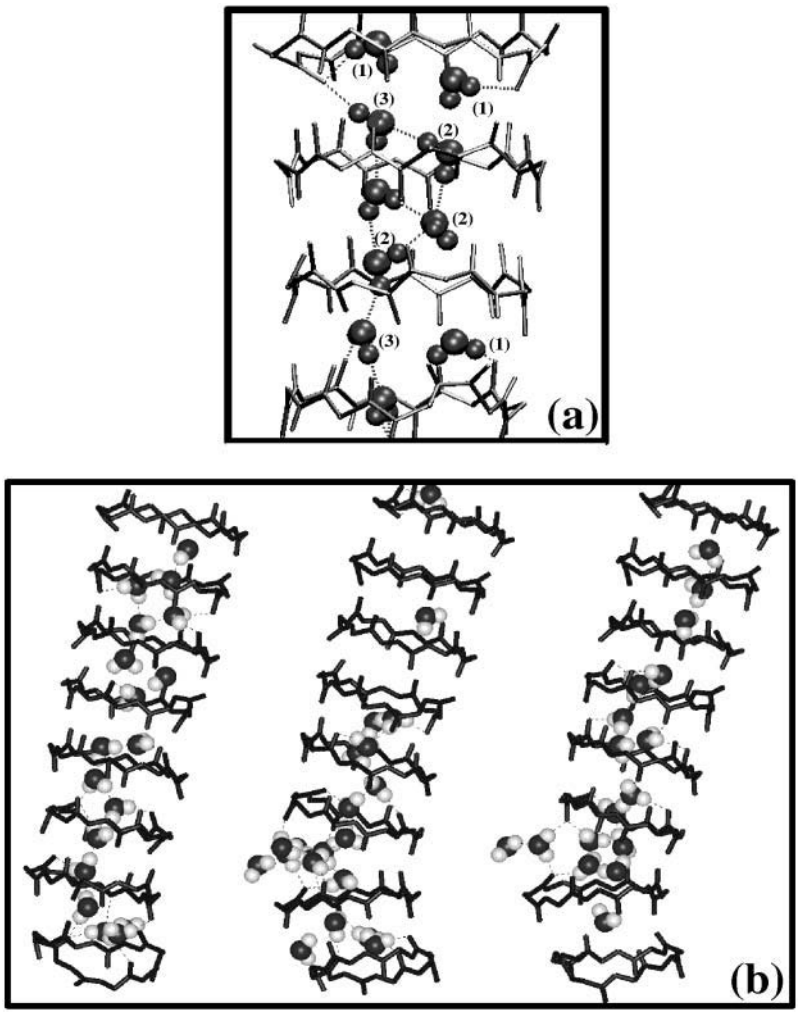

FIGURE 9 Instantaneous configuration of water molecules (rendered in scaled atomic van der Waals radii) inside the synthetic channel (stick representation; side chains omitted for clarity). (*a*) Water molecules are labeled according to their interaction with the surroundings: (1) Molecules forming hydrogen bonds with the peptide channel only, (2) molecules forming hydrogen bonds with one or more water molecules only, and (3) molecules forming hydrogen bonds with both the peptide subunits and neighboring water molecules. (*b*) Snapshots taken at 2, 4, and 7 ns (from left to right) of the MD run.

Overall, the above results suggest that the cyclic peptide nanotubes would conduct water and ions in a rate commensurate with their radius.

Structural features of the lipid environment

The dimensions of the simulation box have changed drastically from their initial values, showing a lateral compression and an expansion in the direction perpendicular to the lipid bilayer. Examination of the lipid structure has revealed that these changes are only partially related to the reorganization of the lipids surrounding the peptide nanotube. In Fig. 11 *a*, we report the density profiles of the aqueous phase and the constituent groups of the DMPC units. The figure shows that the peaks of the density profiles characterizing the CH_2/CH_3, the ester, the phosphate, and the choline groups are shifted by ~2 Å in each leaflet, resulting in a total expansion of the hydrophobic core of ~4 Å in the z direction, normal to the bilayer.

The structural features of the hydrated DMPC bilayer can be further examined by computing the deuterium order parameters, S_{CD}, of the participating aliphatic chains. This quantity is obtained from NMR of deuterated lipids and is given by the average $S_{CD,i} = 1/2\langle(3\cos^2\chi_i - 1)\rangle$, where χ_i denotes the angle formed by the vector pointing from carbon atom i to the deuterium atom attached to it, and the normal to the bilayer (Seelig and Seelig, 1974). Fig. 11 *b* shows the order parameters for the sn-1 and sn-2 chains of those lipid units close and far from the synthetic channel. This distinction was achieved by considering the nearest 52 DMPC molecules out of a total of 215. The order parameters averaged over all lipids are also plotted for comparison purposes. Overall, the order parameters of the hydrocarbon chains progressively increases with time. Fig. 11 *b* reveals only very minor differences between DMPC units close and far from the synthetic channel, i.e., within the expected statistical error, thereby ruling out the concept of ''boundary lipids'' in the vicinity of the nanotube. Whereas the profiles characterizing the early stages of the MD simulation indicate a somewhat lesser order for those lipids close to the nanotube as a result of the nonoptimal packing of the lipid chains around the cylindrical structure, the order parameters of the

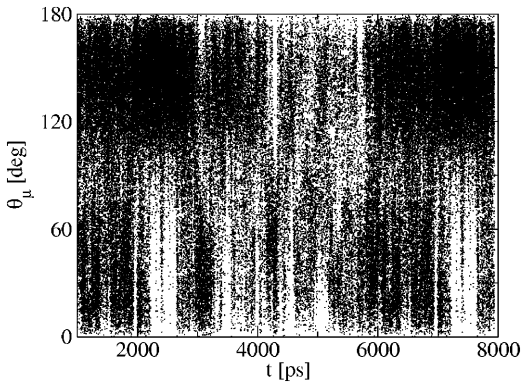

FIGURE 10 Time evolution of angle θ_μ formed by the dipole moment borne by each water molecule present in the peptide channel, and the longitudinal axis of the latter. Only those molecules whose oxygen atom lies between the two planes formed respectively by the third and the eighth cyclic peptides are considered. Note the apparent collective reorientation from parallel ($0 \leq \theta_\mu \leq 60°$) to antiparallel ($120 \leq \theta_\mu \leq 180°$) orientation of the water dipoles.

lipids lying near or far from the synthetic channel are roughly similar toward the end of the trajectory. An MD simulation of less than 2 ns would not have permitted a full relaxation of the lipid chains, hence giving the erroneous impression that the channel might disorder the nearby DMPC units. This suggests that an incomplete sampling is likely to be a source of misinterpreted observations. The increased disorder of lipids located in the vicinity of a membrane protein has been witnessed in a number of recent investigations, including that of the *Mycobacterium tuberculosis* MscL channel (Elmore and Dougherty, 2001), the *Influenza* A virus M_2 protein (Husslein et al., 1998), and the *Escherichia coli* OmpF trimer (Tieleman et al., 1998). In light of the MD simulations performed, it was generally concluded that the membrane protein induces a noteworthy disorder in those lipid units bordering it. In sharp contrast, an opposite tendency was observed in gramicidin A, for which the order of the bound lipid chains was always higher than that of lipids lying further away (Chiu et al., 1999; Roux, 2002). Whereas the nature of the protein undoubtedly affects the nearby lipid chains, and, hence, might rationalize this apparent disagreement, how order parameters evolve with time remains a pivotal issue that requires extensive sampling to be addressed in a convincing way.

The interactions of the lipid molecules with the nanotube may be classified as hydrophobic and hydrogen-bondlike. To investigate the interactions of the synthetic channel with the bilayer interface, we have monitored the hydrogen bonding interactions between the residues of the nanotube and the neighboring DMPC units. Analysis of the 8-ns trajectory reveals the existence of mainly two types of long-lived hydrogen bonds, viz. those formed between the oxygen atoms of the phosphate groups and the L-Trp (i.e., indole NH moiety) or the L-Gln (i.e., amide group) residues, and those formed by the oxygen atoms of the lipid carbonyl and the L-Trp or L-Gln residues. The frequency at which these bonds form and their lifetimes are depicted in Fig. 12. Several lipids form long-lived hydrogen bonds, viz. typically up to several nanoseconds. The lipids appear to be anchored via hydrogen bonds between the oxygen atoms of the phosphate groups and those L-Gln residues located in the first and the last peptide rings, i.e., on both sides of the membrane. Other lipids are hydrogen-bonded to the L-Gln residues located in the two outermost rings through the oxygen atoms of their carbonyl moieties. The most frequent hydrogen-bonding interactions involve, however, the carbonyl groups of the lipid esters and the indole N–H moieties of the L-Trp residues (viz. six per cyclic peptide) located in the last 2 to 3 rings of the synthetic channel, on each side of the membrane. This result is very similar to that found for the gramicidin channel embedded in a lipid membrane (Woolf and Roux, 1994; Roux, 2002). This may underline the importance of L-Trp in mediating the interactions of the peptide with the surrounding lipids, hence participating in the overall stabilization of the channel. NMR data suggest that specific hydrogen bonding interactions of L-Trp residues may not constitute the sole physical basis for the interfacial preference (Yau et al., 1998). Rather, the preference is dominated by the L-Trp flat rigid shape that limits access to the hydrophobic core and its π electron cloud and associated quadrupole moment that favors residing in the interface. In the present case, the nanotube is decorated all along the channel with L-Trp residues. Despite the specific hydrogen bonding interactions of L-Trp residues with the lipid headgroups, the final conformation of the channel results from a balance of more complex interactions with the lipid membrane, where the L-Trp may not play as an important role in the anchoring of the peptide assembly, compared to other systems such as gramicidin A.

CONCLUDING REMARKS

The structural features and the dynamical properties of a synthetic channel formed by eight cyclic peptides of sequence *cyclo*[(L-Trp-D-Leu)$_3$-L-Gln-D-Leu], embedded in a fully hydrated DMPC bilayer were investigated in an 8-ns, large-scale MD simulation. Detailed analysis of the trajectory reveals that the constituent peptide subunits of the antiparallel, β-sheetlike, cylindrical structure remain stacked by means of a robust network of intersubunit backbone-backbone hydrogen bonds between carbonyl, C=O, and amino, N–H, groups. In agreement with ATR-IR spectroscopy measurements, the present simulation shows that the nanotube is tilted with respect to the normal of the water-bilayer interface. The overall tilt of the channel is somewhat smaller than that estimated from IR measurements. It is not clear whether this is mainly due to an inappropriate number of rings considered. A control simulation with a nanotube containing seven and nine rings would be necessary to

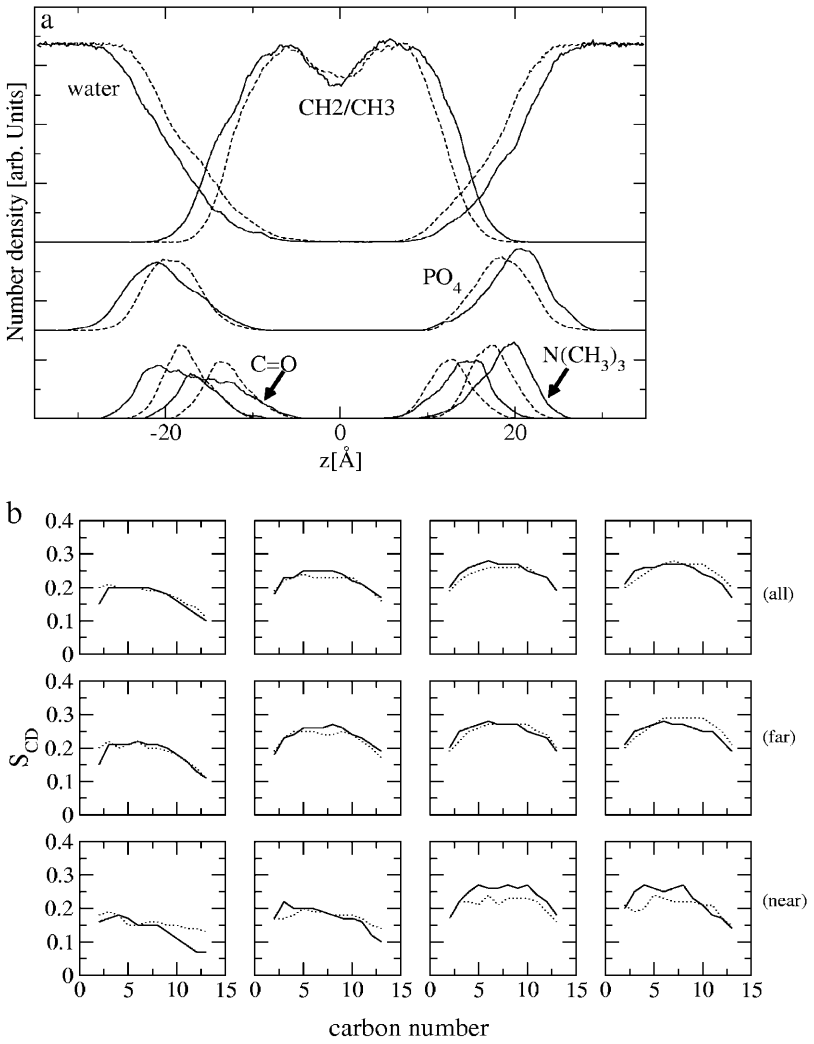

FIGURE 11 (*a*) Density profiles of water and the CH_2/CH_3, the ester, the phosphate and the choline moieties of the DMPC bilayer at the beginning, past a period of 800 ps of equilibration (*dashed lines*), and at the end (*solid lines*) of the MD simulation. Each set of profiles was obtained from time-averages over 800 ps. (*b*) Order parameters of the sn-1 (*solid lines*) and the sn-2 (*broken lines*) hydrocarbon chains of the hydrated DMPC bilayer, averaged over 200 ps, and estimated ~1, 3, 5, and 7 ns of the MD run (from left to right panel). Distinction is being made between those lipid units closely and remotely located from the synthetic channel. Order parameters characteristic of the DMPC units near the nanotube are obtained from averages over a subset of the nearest 52 lipids, out of a total of 215 lipids.

clarify this point. Single conductance measurements reveal that for a given cyclic peptide constituent, the number of units forming a channel in a liposome may vary, showing that assembly-disassembly of up to two rings occur within the same system. Accordingly, and emphasizing the fact that the eight cyclic peptide nanotube approximates rather well the IR results, one may consider that the present system is realistic enough to allow the study of the properties of the channel/membrane assembly.

The overall tilt of the channel reproduced by the simulation is accompanied by an expansion of the hydrophobic thickness of the lipid bilayer. Any or both effects are likely to constitute the response of the system for overcoming the initial hydrophobic mismatch due to the greater length of the nanotube compared to the thickness of a bare DMPC bilayer. This is similar to what has been observed and discussed in greater detail for model peptides (de Planque et al., 2001; Petrache et al., 2002). Another feature observed here, and commonly reported for membrane proteins, is the specific interaction of L-Trp residues with the membrane interface, which seems to play an important role in the anchoring of the transmembrane domains and, therefore, in the final channel/bilayer conformation (Tieleman et al., 1998; Yau et al., 1998; Ridder et al., 2000; de Planque et al., 2002; van der Wel et al., 2002). From a biological perspective, the anchoring and the tilt of the channel as well as the adaptation of the supporting membrane appear to be, in contrast with other systems, of lesser importance for cyclic peptide nanotubes. One crucial feature of such channels lies in their capability to adjust their length through the number of cyclic units, thereby adapting to their host membrane (Ghadiri et al., 1994) and functioning in a rather similar way regardless of the specific length of the membrane. Hence, the hydrophobic mismatch that may play a critical role in the function of the guest transmembrane proteins, e.g., in gramicidin A (Martinac and Hamill, 2002), appears to be not as discriminatory for cyclic peptide channels.

Although there is no clear-cut mechanism for rationalizing the sudden and partial dislocation of the synthetic channel after ~3 ns, it may be inferred that it is a transient phenomenon, part of a dynamic process. During the simulation, we observe a breakdown of the hydrogen bond network

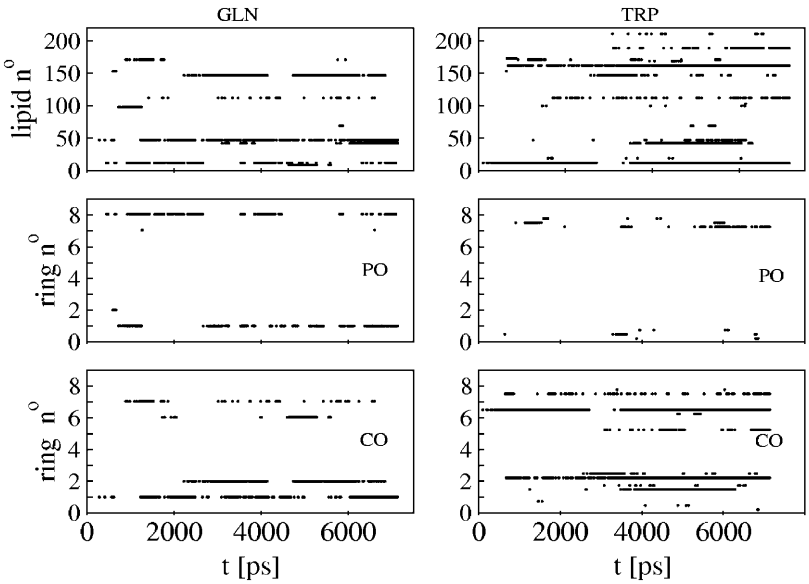

FIGURE 12 Time evolution of hydrogen bonds (HB) between the lipid membrane molecules and specific residues (Gln on left panels and Trp on right panels) of the peptide nanotubes. From top to bottom: HB between lipids and the peptide residues (molecule number on the *y* axis), HB between the phosphate oxygen atoms and the peptide residue, and HB between the carbonyl oxygen atoms and the specific residues, respectively (ring number to which the peptide residue belongs reported on the *y* axis).

connecting two rings. After this, some internal water molecules confined near the collapse region reside for long periods of time holding the rings through hydrogen bonds. The resulting channel configuration may have consequences on ion transport properties. Peptide channel gating was observed experimentally through single-channel conductance measurements (Ghadiri et al., 1994; Clark et al., 1998). The lifetimes of observed ''open'' and ''closed'' transitions in liposomes depend on the peptide-to-lipid concentration and range in the ms timescale (Ghadiri et al., 1994), which is beyond the timescale reachable by MD simulation. The sharp transitions in the measured voltage, indicative of a gating mechanism, were tentatively ascribed to conformational changes, or assembly-disassembly of the channel structure. The disorder of the nanotube herein observed might constitute a preliminary step for such a possible disassembly process.

From a biological perspective, the present MD study provides a glimpse of the complex interactions of the peptide nanotube with the lipid bilayer, which, assuming an appropriate sequence of amino acids, will ultimately trigger severe modifications of the permeability properties of the bacterial membrane (Fernandez-Lopez et al., 2001). Whereas the mode of permeation investigated herein offers a lesser membrane discrimination and most likely a reduced in vitro activity than the so-called ''carpetlike'' mode, it nonetheless illuminates how the presence of a synthetic channel formed by stacked cyclic peptides affects the characteristics of the lipid bilayer. An important characteristic of the synthetic channel when assembled in the membrane lies in its permeation properties, allowing water molecules to flow along the hollow cylindrical structure. The analysis of the water structure inside the nanotube has revealed several features in common with other protons and water transporters. The existence of water wires and preferred orientations of water molecules suggest a proton transfer mechanism similar to that suggested for gramicidin A (Roux, 2002). Concerning water transport within the channel, the analysis of the water molecular diffusion and estimates of the channel conductance suggest that cyclic peptide channels could allow the passage of small ions across the membrane, with rates commensurate with their internal sections, modulating accordingly transmembrane potentials. A more thorough study targeted at examining the assisted transport of cations through a homologous antiparallel, β-sheetlike channel in the presence of an external electric field would be more informative about the detailed conductance process; this study is currently in progress.

The authors are grateful to Reza Ghadiri for insightful comments on the preliminary results.

We thank the Centre National de la Recherche Scientifique (CNRS) for the *poste rouge* and the ATIP: Action Thématique et Incitative sur Programme Grant of M.T. The Centre Charles Hermite (CCH), Vandœuvre-lès-Nancy, France, and the CINES: Centre Informatique National de l'Enseignement Supérieur, Montpellier, France, are gratefully acknowledged for provision of generous amounts of CPU time on their SGI Origin 2000 and Origin 3800.

REFERENCES

Andersen, H. C. 1983. Rattle: a velocity version of the SHAKE algorithm for molecular dynamics calculations. *J. Comput Phys.* 52:24–34.

Arseniev, A. S., I. L. Barsukov, V. F. Bystrov, A. L. Lomize, and Y. A. Ovchinnikov. 1985. 1H-NMR study of gramicidin A transmembrane ion channel. Head-to-head, right-handed, single-stranded helices. *FEBS Lett.* 186:168–174.

Asthagiri, D., and D. Bashford. 2002. Continuum and atomistic modeling of ion partitioning into a peptide nanotube. *Biophys. J.* 82:1176–1189.

Bacon, D. J., and W. F. Anderson. 1988. A fast algorithm for rendering space-filling pictures. *J. Mol. Graph.* 6:219–220.

Bernèche, S., and B. Roux. 2000. Molecular dynamics of KcsA K^+ channel in a bilayer membrane. *Biophys. J.* 78:2900–2917.

Bhandarkar, M., R. Brunner, C. Chipot, A. Dalke, S. Dixit, P. Grayson, J. Gullinsrud, A. Gursoy, W. Humphrey, D. Hurwitz, N. Krawetz, M. Nelson, J. Phillips, A. Shinozaki, G. Zheng, and F. Zhu. 2002. NAMD version 2.4. *http://www.ks.uiuc.edu/Research/namd.*

Bong, D. T., T. D. Clark, J. R. Granja, and M. R. Ghadiri. 2001. Self-assembling organic nanotubes. *Angew. Chem. Int. Ed. Engl.* 40:988–1011.

Chiu, S. W., S. Subramanian, and E. Jakobsson. 1999. Simulation study of a gramicidin/lipid bilayer system in excess water and lipid. II. Rates and mechanisms of water transport. *Biophys. J.* 76:1939–1950.

Clark, T. D., L. K. Buehler, and M. R. Ghadiri. 1998. Self-assembling cyclic β^3-peptide nanotubes as artificial transmembrane ion channels. *J. Am. Chem. Soc.* 120:651–656.

Cragg, P. J. 2002. Artificial transmembrane channels for sodium and potassium. *Sci. Prog.* 85:219–241.

Darden, T., D. York, and L. Pedersen. 1993. Particle mesh Ewald: an Nlog(N) method for Ewald sums in large systems. *J. Chem. Phys.* 98:10089–10092.

De Groot, B. L., and H. Grubmüller. 2001. Water permeation across biological membranes: mechanism and dynamics of aquaporin-1 and GlpF. *Science.* 294:2353–2357.

de Planque, M. R. R., J. W. P. Boots, D. T. S. Rijkers, R. M. J. Liskamp, D. V. Greathouse, and J. A. Killian. 2002. The effect of hydrophobic mismatch between phosphatidylcholine bilayers and transmembrane alpha-helical peptides depend on the nature of interfacially exposed aromatic and charged residues. *Biochemistry.* 41:8396–8404.

de Planque, M. R. R., E. Goormaghtigh, D. V. Greathouse, R. E. Koeppe II, J. A. W. Kruijtzer, R. M. J. Liskamp, B. de Kruijff, and J. A. Killian. 2001. Sensitivity of single membrane-spanning alpha-helical peptides to hydrophobic mismatch with a lipid bilayer: effects on backbone structure, orientation, and extent of membrane incorporation. *Biochemistry.* 40:5000–5010.

Elmore, D. E., and D. A. Dougherty. 2001. Molecular dynamics simulations of wild-type and mutant forms of the Mycobacterium tuberculosis MscL channel. *Biophys. J.* 81:1345–1359.

Engels, M., D. Bashford, and M. R. Ghadiri. 1995. Structure and dynamics of self-assembling peptide nanotubes and the channel-mediated water organization and self-diffusion. A molecular dynamics study. *J. Am. Chem. Soc.* 117:9151–9158.

Essmann, U., L. Perera, M. L. Berkowitz, T. Darden, and L. G. Pedersen. 1995. A smooth particle mesh Ewald method. *J. Chem. Phys.* 103:8577–8593.

Feller, S. E., D. Huster, and K. Gawrisch. 1999. Interpretation of NOESY cross-relaxation rates from molecular dynamics simulation of a lipid bilayer. *J. Am. Chem. Soc.* 121:8963–8964.

Fernandez-Lopez, S., H.-S. Kim, E. C. Choi, M. Delgado, J. R. Granja, A. Khasanov, K. Kraehenbuehl, G. Long, D. A. Weinberger, K. M. Wilcoxen, and M. R. Ghadiri. 2001. Antibacterial agents based on the cyclic D,L-alpha-peptide architecture. *Nature.* 412:452–455.

Forrest, L. R., A. Kukol, I. T. Arkin, D. P. Tielman, and M. S. P. Sansom. 2000. Exploring models of the influenza A M2 channel: MD simulations in a phospholipid bilayer. *Biophys. J.* 78:55–69.

Ghadiri, M. R., J. R. Granja, and L. Buehler. 1994. Artificial transmembrane ion channels from self-assembling peptide nanotubes. *Nature.* 369:301–304.

Ghadiri, M. R., J. R. Granja, R. A. Milligan, D. E. McRee, and N. Khazanovich. 1993. Self-assembling organic nanotubes based on a cyclic peptide architecture. *Nature.* 366:324–327.

Granja, J. R., and M. R. Ghadiri. 1994. Channel-mediated transport of glucose across lipid bilayers. *J. Am. Chem. Soc.* 116:10785–10786.

Hartgering, J. D., J. R. Granja, R. A. Milligan, and M. R. Ghadiri. 1996. Self-assembling peptide nanotubes. *J. Am. Chem. Soc.* 118:43–50.

Hummer, G., J. C. Rasaiah, and J. P. Noworyta. 2001. Water conduction through the hydrophobic channel of a carbon nanotube. *Nature.* 414:188–190.

Husslein, T., P. B. Moore, Q. F. Zhong, D. M. Newns, P. C. Pattnaik, and M. L. Klein. 1998. Molecular dynamics simulation of a hydrated diphytanol phosphatidylcholine lipid bilayer containing an αlpha-helical bundle of four transmembrane domains of the influenza A virus M2 protein. *Faraday Disc.* 111:201–208.

Izaguirre, J. A., D. P. Catarello, J. M. Wozniak, and R. D. Skeel. 2001. Langevin stabilization of molecular dynamics. *J. Chem. Phys.* 114:2090–2098.

Izaguirre, J. A., S. Reich, and R. D. Skeel. 1999. Longer time steps for molecular dynamics. *J. Chem. Phys.* 110:9853–9864.

Kale, L., R. Skeel, M. Bhandarkar, R. Brunner, A. Gursoy, N. Krawetz, J. Phillips, A. Shinozaki, K. Varadarajan, and K. L. Schulten. 1999. NAMD2: Greater scalability for parallel molecular dynamics. *J. Comput. Phys.* 151:283–312.

Ketchem, R. R., B. Roux, and T. Cross. 1997. High-resolution refinement of a solid-state NMR-derived structure of gramicidin A in a lipid bilayer environment. *Structure.* 5:1655–1669.

Khazanovich, N., J. R. Granja, D. E. McRee, R. A. Milligan, and M. R. Ghadiri. 1994. Nanoscale tubular ensembles with specified internal diameters. Design of a self-assembled nanotube with a 13-A pore. *J. Am. Chem. Soc.* 116:6011–6012.

Kim, H. S., D. Hartgerink, and M. R. Ghadiri. 1998. Oriented self-assembly of cyclic peptide nanotubes in lipid membranes. *J. Am. Chem. Soc.* 120:4417–4424.

Kong, Y., and J. Ma. 2001. Dynamical mechanisms of the membrane water channel aquaporin-1 (AQP1). *Proc. Natl. Acad. Sci. USA.* 98:14345–14349.

König, S., and E. Sackmann. 1996. Molecular and collective dynamics of lipid bilayers. *Curr. Opin. Colloid Interface Sci.* 1:78–82.

Kraulis, P. 1991. MOLSCRIPT: A program to reproduce both detailed and schematic plots of protein structures. *Journal of Applied Crystallography.* 24:946–950.

Law, R. J., D. P. Tieleman, and M. S. P. Sansom. 2003. Pores formed by the nicotinic receptor m2delta peptide: a molecular dynamics simulation study. *Biophys. J.* 84:14–27.

MacKerell, A. D., Jr., D. Bashford, M. Bellott, R. L. Dunbrack, Jr., J. Evanseck, M. J. Field, S. Fischer, J. Gao, H. Guo, S. Ha, D. Joseph-McCarthy, L. Kuchnir, K. Kuczera, F. T. K. Lau, C. Mattos, S. Michnick, T. Ngo, D. T. Nguyen, B. Prodhom, W. E. Reiher III, B. Roux, M. Schlenkrich, J. C. Smith, R. Stote, J. Straub, M. Watanabe, J. Wiorkiewicz-Kuczera, D. Yin, and M. Karplus. 1998. All-atom empirical potential for molecular modeling and dynamics studies of proteins. *J. Phys. Chem. B.* 102:3586–3616.

Martinac, B., and O. P. Hamill. 2002. Gramicidin A channels switch between stretch activation and stretch inactivation depending on bilayer thickness. *Proc. Natl. Acad. Sci. USA.* 99:4309–4312.

Martyna, G. J., M. E. Tuckerman, D. J. Tobias, and M. L. Klein. 1996. Explicit reversible integrators for extended systems dynamics. *Molec. Phys.* 87:1117–1157.

Matile, S. 2001. En route to supramolecular functional plasticity: artificial beta-barrels, the barrel-stave motif, and related approaches. *Chem. Soc. Rev.* 30:158–167.

Merritt, E. A., and M. E. P. Murphy. 1994. RASTER3D version 2.0: a program for photorealistic molecular graphics. *Acta Crystallogr. D.* 50:869–873.

Motesharei, K., and M. R. Ghadiri. 1997. Diffusion-limited size-selective ion sensing based on SAM-supported peptide nanotubes. *J. Am. Chem. Soc.* 119:11306–11312.

Petrache, H. I., S. Tristan-Nagle, and J. F. Nagle. 1998. Fluid phase structure of EPC and DMPC bilayers. *Chem. Phys. Lipids.* 95:83–94.

Petrache, H. I., D. M. Zuckerman, J. N. Sachs, J. A. Killian, R. E. Koeppe II, and T. B. Woolf. 2002. Hydrophobic matching mechanism in-

vestigated by molecular dynamics simulations. *Langmuir*. 18:1340–1351.

Pomès, R., and B. Roux. 2002. Molecular mechanism of H^+ conduction in the single-file water chain of the gramicidin channel. *Biophys. J*. 82: 2304–2316.

Ridder, A. N., S. Morein, J. G. Stam, A. Kuhn, B. de Kruijff, and A. J. Killian. 2000. Analysis of the role of interfacial tryptophan residues in controlling the topology of membrane proteins. *Biochemistry*. 39:6521–6528.

Roux, B. 2002. Computational studies of the gramicidin channel. *Acc. Chem. Res*. 35:366–375.

Ryckaert, J.-P., G. Ciccotti, and H. J. C. Berendsen. 1977. Numerical integration of the cartesian equations of motion of a system with constraints: molecular dynamics of *n*-alkanes. *J. Comput. Phys*. 23:327–341.

Seelig, A., and J. Seelig. 1974. Dynamic structure of fatty acyl chains in a phospholipid bilayer measured by deuterium magnetic resonance. *Biochemistry*. 13:4839–4845.

Shrivastava, I. H., and M. S. P. Sansom. 2000. Simulations of ion permeation through a potassium channel: molecular dynamics of KcsA in a phospholipid bilayer. *Biophys. J*. 78:557–570.

Smart, O. S., J. Breed, G. R. Smith, and M. S. P. Sansom. 1997. A novel method for structure-based prediction of ion channel conductance properties. *Biophys. J*. 72:1109–1126.

Smart, O. S., G. M. P. Coates, M. S. P. Sansom, G. M. Alder, and C. L. Bashford. 1998. Structure-based prediction of the conductance properties of ion channels. *Faraday Discuss*. 111:185–199.

Smart, O. S., J. M. Goodfellow, and A. Wallace. 1993. The pore dimensions of gramicidin A. *Biophys. J*. 65:2455–2460.

Tajkhorshid, E., P. Nollert, M. O. Jensen, L. J. W. Miercke, J. O'Connell, R. M. Stroud, and K. Schulten. 2002. Control of the selectivity of the aquaporin water channel family by global orientational tuning. *Science*. 296:525–530.

Tieleman, D. P., P. C. Biggin, G. R. Smith, and M. S. P. Sansom. 2001. Simulation approaches to ion channel structure-function relationships. *Q. Rev. Biophys*. 34:473–561.

Tieleman, D. P., L. R. Forrest, M. S. P. Sansom, and H. J. C. Berendsen. 1998. Lipid properties and the orientation of aromatic residues in OmpF, influenza M2, and alamethicin systems: molecular dynamics simulations. *Biochemistry*. 37:17544–17561.

van der Wel, P. C., E. Strandberg, J. A. Killian, and R. E. Koeppe II. 2002. Geometry and intrinsic tilt of a tryptophan-anchored transmembrane alpha-helix determined by (2)H NMR. *Biophys. J*. 83:1479–1488.

Woolf, T. B., and B. Roux. 1994. Molecular dynamics simulation of the gramicidin channel in a phospholipid bilayer. *Proc. Natl. Acad. Sci. USA*. 91:11631–11635.

Yang, Y., D. Henderson, P. Crozier, R. L. Rowley, and D. D. Busath. 2002. Permeation of ions through a model biological channel: effect of periodic boundary conditions and cell size. *Molec. Phys*. 100:3011–3019.

Yau, W.-M., W. C. Wimley, K. Gawrisch, and S. H. White. 1998. The preference of tryptophan for membrane interfaces. *Biochemistry*. 37:14713–14718.

Zhong, Q., Q. Jiang, P. B. Moore, D. M. Newns, and M. L. Klein. 1998. Molecular dynamics simulation of a synthetic ion channel. *Biophys. J*. 74:3–10.

Zhu, F., E. Tajkhorshid, and K. Schulten. 2001. Molecular dynamics study of aquaporin-1 water channel in a lipid bilayer. *FEBS Lett*. 504:212–218.